HELIOSPHERE-GEOSPHERE INTERACTIONS USING LOW ENERGY NEUTRAL ATOM IMAGING

T.E. MOORE[1], M.R. COLLIER[1], M.-C. FOK[1], S.A. FUSELIER[2], H. KHAN[1], W. LENNARTSSON[2], D.G. SIMPSON[1], G.R. WILSON[3] and M.O. CHANDLER[4]

[1]*NASA's Goddard Space Flight Center, Interplanetary Physics Branch, Code 692, Greenbelt, MD 20771, USA*
[2]*Lockheed Martin Advanced Technology Center, Dept. H1-11, Bldg. 255, Palo Alto, CA 94304, USA*
[3]*Mission Research Corporation, 589 W. Hollis St., Suite 201, Nashua, NH 03062, USA*
[4]*National Space Science and Technology Center, NASA MSFC SD50, Huntsville AL 35805, USA*

Abstract. Development of the low energy neutral atom (LENA) imager was originally motivated by a need to remotely sense plasma heating in the topside ionosphere, with the goal of greatly enhanced temporal resolution of an otherwise familiar phenomenon. During ground test and calibration, the LENA imager was found to respond to neutral atoms with energies well above its nominal energy range of 10–750 eV, up to at least 3–4 keV, owing to sputtering interactions with its conversion surface. On orbit, LENA has been found to respond to a ubiquitous neutral atom component of the solar wind, to the neutral atoms formed by magnetosheath interactions with the geocorona during periods of high solar wind pressure, and to the interstellar neutral atoms flowing through the heliosphere during the season of maximal relative wind velocity between spacecraft and interstellar medium. LENA imaging has thus emerged as a promising new tool for studying the interplanetary medium and its interaction with the magnetosphere, in addition to the ionospheric heating and outflow that result from this interaction. LENA emissions from the ionosphere consist of a fast component that can be observed at high altitudes, and slower components that evidently create a quasi-trapped extended superthermal exosphere. The more energetic emissions are responsive to solar wind energy inputs on time scales of a few minutes.

1. Low Energy Neutral Atom Imaging

Ordinary heliospheric and geospheric gases are ionized mainly by energetic photon or particle interactions, rather than by thermal heating. One probable exception, the solar corona, is heated by mechanisms that remain somewhat mysterious (e.g., Scudder, 1992). Consequently, heliospheric plasmas are for the most part partially ionized gases, rather than fully ionized plasmas, even where their densities are so low that collision scale lengths are larger than the system in which they reside. Ions and atoms exchange charge with a cross section much larger than that for scattering or momentum transfer, so it is common for nuclei of coexisting plasma ions and neutral gas atoms to spend part of their time as atoms and part of their time as ions. As ions, these nuclei are subject to a variety of electromagnetic processes that heat or accelerate them to energies higher (sometimes many orders of magnitude higher) than that of the thermal neutral gas from which they sprang. The same electromagnetic forces that heat or accelerate nuclei while they are ions, may also

entrap the high speed ions, as in a magnetosphere. Then any charge exchange back to the atomic gas state allows the high speed atom to very rapidly escape from the system in which it was trapped, giving rise to a glow of fast escaping atoms from any hot plasma population that is trapped in coexistence with a neutral atom population. This in turn makes possible remote sensing of the hot plasma using an energetic neutral atom camera of suitable design, of which three are found on the IMAGE spacecraft (Burch *et al.*, 2001).

Energetic Neutral Atom (ENA) imaging can thus be described in terms that generalize downward in energy all the way to the core components of the gas and the plasma. This was the goal of the development of the Low Energy Neutral Atom (LENA) imager for the IMAGE mission. That is, the LENA imager was designed to observe those neutral atoms having energies within one or two decades of the thermal gas, the goal being to make remote observations of the initial stages of plasma heating known to occur in the topside ionosphere of the Earth. Such heating is also known to give rise to substantial plasma outflows from their normal gravitational trap in the topside ionosphere, a phenomenon that has been studied for some decades *in situ* (Moore, Lundin *et al.*, 1999), but which has proved somewhat resistant to a detailed understanding of its causes and spatial/temporal distribution. The time required to build up a global picture of this phenomenon from *in situ* measurements is on the order of spacecraft orbital precession periods, so that it has been impossible to study it on short time scales relevant to the dynamics of helio-spheric structures interacting with the geosphere. LENA imaging seeks to remotely sense this plasma heating, so that its variations can be resolved in much more detail. Initial results from the Swedish Astrid spacecraft have been encouraging in this regard (Brandt *et al.*, 2001)

The energy range of interest here is from the oxygen gravitational binding energy ($\leqslant 10$ eV; implying that the lowest energy fast oxygen atoms will be strongly influenced by gravity), up to the energy at which atoms can penetrate thin carbon foils ($\geqslant 1$ keV), at which point they become detectable using that technique to identify their passage (Pollock *et al.*, this volume; Mitchell *et al.*, this volume). The LENA imager solves the problem of detecting and analyzing fast neutral atoms that will not pass through foils or emit secondary electrons from surfaces using a process closely related to the creation of the fast atoms, namely charge transfer (Moore *et al.*, 2000). Charge transfer is used to convert the incident atoms into ions that can then be analyzed using conventional electrostatic optics and time-of-flight techniques. To assure maximal probability of charge transfer interactions, incoming neutral atoms are incident upon a conical polished conversion surface at grazing incidence, from which they are reflected in a nearly specular angular pattern, while acquiring an electron and thus becoming negative ions with energy on average equal to $\sim 60\%$ of incident particle energy. The LENA imager electro-static optics provides for the detection and analysis into three broad energy bins of negative ions leaving the conversion surface with energies between about 10 and 350 eV in its default operating configuration. A "steering voltage" can be used to

raise this overall energy range to about 20 to 700 eV. The reflection process suffers from appreciable angular dispersion, limiting the angular resolution that can be obtained in the imaging direction to about 15°. The nominal field of view measures 90° wide, with the Earth at the center of the 90° direction. Spacecraft spin sweeps this FOV around a full 360° once in 2 minutes. The overall detection efficiency is approximately 1% and increases significantly with energy.

In addition to conversion (charge transfer) interactions, sputtering of conversion surface atoms occurs for incident particles whose energy exceeds a few 100 eV for hydrogen, and somewhat lower for heavier species. An appreciable fraction of sputtered atoms are in the negative ion state that can be analyzed by the ESA optics and detection system and are therefore useful to provide a higher energy response range, and a response to He atoms, which cannot be converted to negative ions with useful lifetimes. The sputtered ions have energies a fraction of the incident atoms, and their angular emission pattern is clearly somewhat broader than for converted (charge transfer) atoms. Nevertheless, this sputter process means that LENA has an energy range up to a few keV when the ion optics is set for a range up to 350 eV. This has allowed the LENA imager to make observations of not only the fast atom emissions from the Earth, but also a neutral atom component of the solar wind, and the low energy part of the ring current plasmas. Finally, the LENA imager has successfully detected the interstellar neutral gas streaming through the solar system, and in particular, a feature resembling the focusing cone that exists in the downstream direction from the sun (Lallement, 1999).

In following sections, we summarize the lessons learned to date from our experience with the LENA imager in the areas of neutral solar wind, geospheric fast neutral atom emission, and interstellar gas and dust in the heliosphere.

2. Neutral Solar Wind

2.1. NEUTRAL ATOM SOLAR WIND

Because the solar atmosphere is fully ionized (typically 1 neutral atom in about 10^7) in the solar corona (Arnaud and Rosenflug, 1985), the neutral solar wind results mainly from subsequent charge exchange interactions between solar wind ions (mainly H^+) and the neutral gas column between the Earth and the sun. The interplanetary neutral gas contains three main components: a gas population that is sputtered from interplanetary dust grains (Banks, 1971), interstellar gas flowing through the solar system (Bzowski *et al.*, 1996), and outgassing from the planets, notably the Earth (Rairden *et al.*, 1986).

The first signal observed by the LENA imager when it was activated in May 2000 was a narrow peak in spin angle corresponding to the sector during which the FOV was looking sunward. The LENA imager was designed with great care to reject solar UV light, but this signal was initially interpreted as a UV light
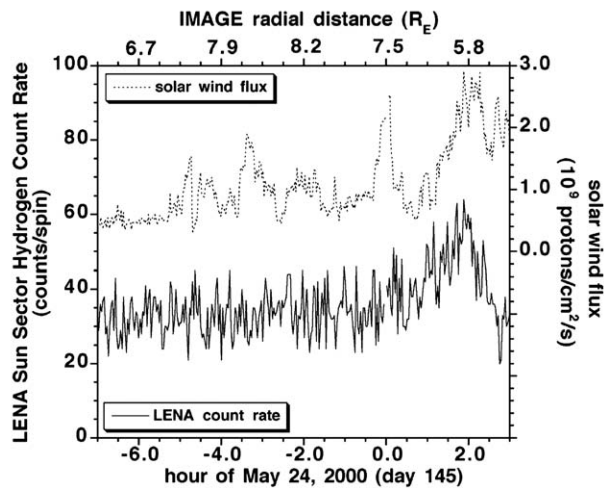
Figure 1. Short term neutral solar wind variations (solid trace, right hand Y axis) related to solar wind flux (dotted trace, right hand Y axis).

leak, because a weak UV response had been experienced during lab testing using a solar UV simulation source. The first indication that this might not be correct was an observation about a month later in which the arrival of a coronal mass ejection at the Earth produced a prompt enhancement of the "sun pulse". Clearly, an enhancement of the relevant solar FUV/EUV spectrum in precise coincidence with a CME arrival would be unlikely, and indeed, this was borne out in a number of tests of the nature of this solar response (Collier *et al.*, 2001). It was shown there:

- that no comparable enhancement of solar UV was observed at the time of enhancements of the LENA sun signal;
- that occasions with increased solar EUV were not accompanied by any perceptible LENA response; and
- that good correlation was seen between the solar wind ion flux and the LENA imager response when viewing in the direction of the sun;
- that a distinct apparent LENA compositional change resulted from abrupt changes in solar wind velocity, consistent with a change in sputtering products from the conversion surface.

In Figure 1 we illustrate some of the short-term variations of the neutral solar wind signal. The figure shows that the LENA response tracks changes in the solar wind on moderate time scales, but not at the shortest time scales. The ENA flux is in general a line of sight integral over a scale length of several charge exchange collision mean free paths in the upstream solar wind. This distance is a strong function of how much geocoronal and-or interstellar material lies sunward of any specific spacecraft location. When the solar wind dynamic pressure is elevated, compressing the magnetosphere, substantially enhanced densities of geocoronal hydrogen are encountered near the Earth, resulting in much shorter mean free paths

and closer tracking of solar wind conditions in the neutral solar wind component, as seen in Figure 1. At times of lower solar wind pressure, the magnetosphere is large and only a small signal comes from geocoronal charge exchange. The neutral solar wind then responds to and averages over distant upstream influences and is quite poorly correlated with their later realizations at the Earth on a fine scale.

2.2. MAGNETOSHEATH AND CUSP STRUCTURE

Another observation was that periods of especially intense solar wind were accompanied by LENA emissions from directions well away from the sun direction itself, presumably owing to these magnetosheath interactions with the sunward geocorona. The first step to investigate this hypothesis was to develop a simulation of the process, to compute the expected fluxes of LENA. The most straightforward path to this goal was to use an MHD simulation of the dayside magnetosheath region in conjunction with a standard geocoronal model. The line-of-sight flux integrals were then carried out using the same tools that have been developed to simulate ring current ENA emissions. The geometry of this situation is illustrated schematically in Figure 2. Here we see a view of the ecliptic plane and its intersection with the bow shock, magnetopause, and showing the orientation of the LENA imager FOV at a time when the spacecraft orbit runs from about 10–22 UT.

Results are based on use of the BatsRUS simulation code (Groth *et al.*, 2000), which can be run at GSFC for specific events. The code computes the local solar wind plasma density, flow velocity and temperature. Substantial heating occurs as the plasma traverses the bow shock, and a realistic hot subsonic magnetosheath results. We computed the line of sight neutral fluxes at specified energies using an isotropic Maxwellian velocity distribution with temperature as specified by the code results. This method limits the results to those appropriate to the thermal solar wind and its interactions with Earth's geocorona, but this gives the main observed features, as shown in Figure 3. Here the neutral atom fluxes have been computed at the IMAGE spacecraft position for two different orbit perspectives, assuming solar wind conditions typical of a CME period with relatively high solar wind density, velocity and dynamic pressure. A sharp peak of the LENA flux is observed and simulated for the noon-midnight orbit, with the upstream solar wind direction well within the LENA imager FOV. When the solar wind direction is beyond the LENA imager FOV, substantial but more diffuse emissions are expected and observed from spin phases at which the LENA imager FOV looks closest to the sun, even when the spacecraft is in a generally dawn-dusk oriented orbit. Thus, these simulation features replicate both the sharp intense spike in the direction toward the sun and the more diffuse glow that originates from the heated and slowed magnetosheath.

In the case of noon-midnight orbit orientation, high dynamic pressure solar wind events are expected to produce widespread LENA emissions as the subsolar magnetopause is compressed to the vicinity of geosynchronous orbit. This is indeed
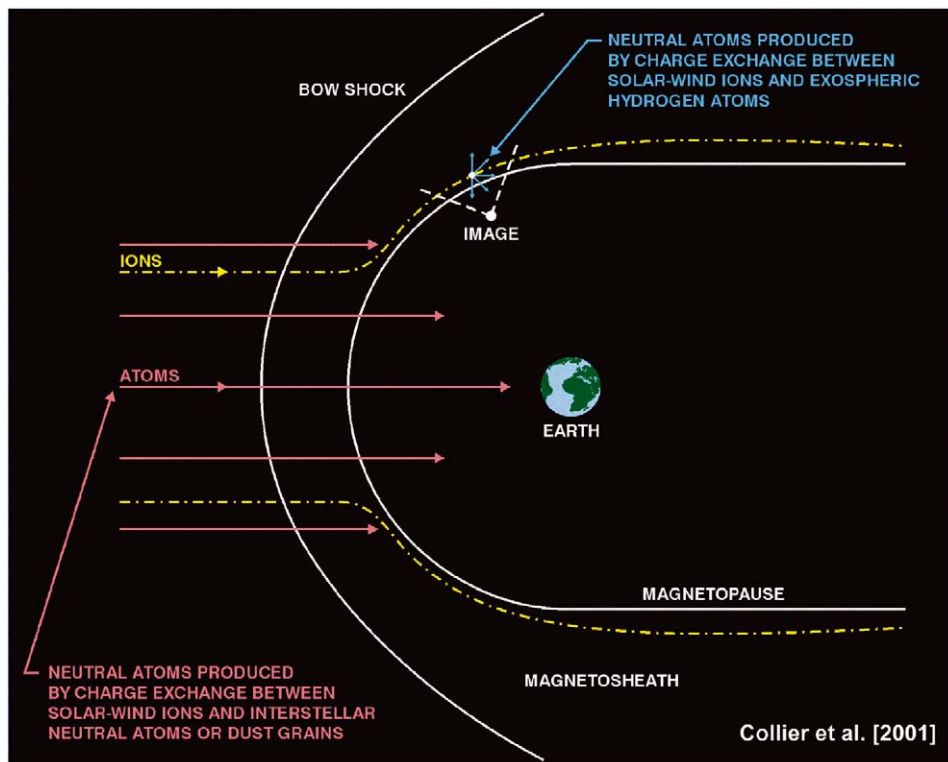
Figure 2. The solar wind interaction with the magnetosphere in ecliptic plane, identifying separate neutral atom populations produced by interactions upstream of the bow shock, and magnetosheath interactions downstream of the bow shock (Collier *et al.*, 2001).

the case, as illustrated in Figure 4, where a LENA flux spin profile is compared with an event simulation from the BatsRUS code running at the GSFC Coordinated Community Modeling Center. The spike in the LENA count rate corresponds to the direct neutral solar wind signal, while the more diffuse count rates correspond to viewing directions as indicated in the diagram of the simulation density distribution. For this event, magnetosheath plasma was observed at geosynchronous orbit (M. Thomsen, personal communication), in qualitative agreement with these simulation results.

The simulation contains discrete structures appearing as density enhancements associated with the magnetospheric cusp entry regions. The LENA data confirm the existence of similar structures in the line-of-sight integrations of LENA emission from these regions. It is not always possible to monitor the magnetosheath region, but it becomes increasingly practical during times of elevated solar wind dynamic pressure. It can be seen that features of the LENA flux profile correspond closely to the simulated structure of the magnetosheath on this day, in particular reproducing
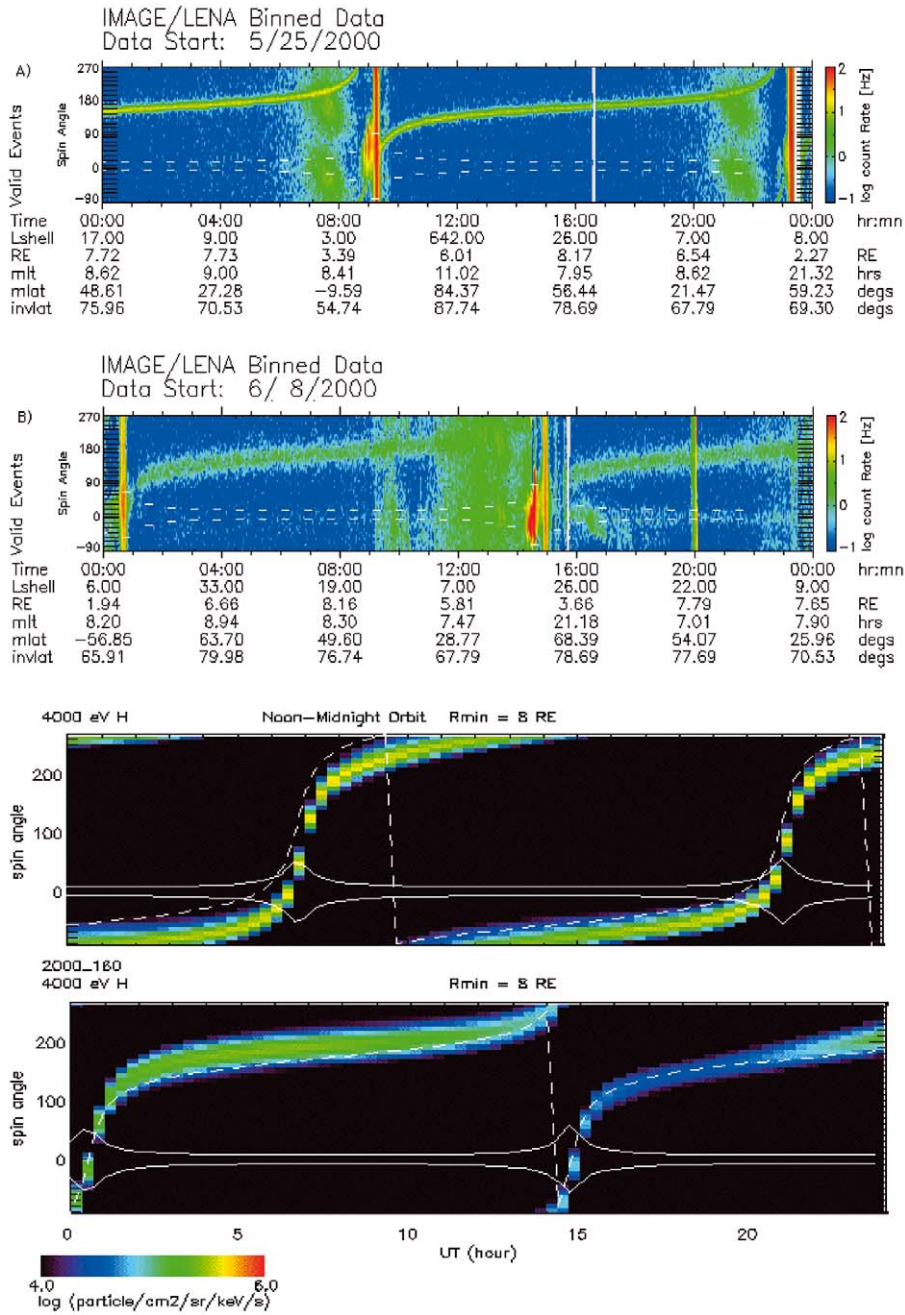
Figure 3. Comparison of typical LENA imager observations (left column) with simulations of LENA fluxes for 4000 eV protons (right column), from dawn-dusk (top) and noon-midnight (bottom) orbits. Line of sight integrals run from 8 R$_E$ to 50 R$_E$. Solid white lines mark the limbs of the Earth. The dashed white line marks the spin phase at which the Sun has the smallest latitude angle from the center of the LENA field of view.
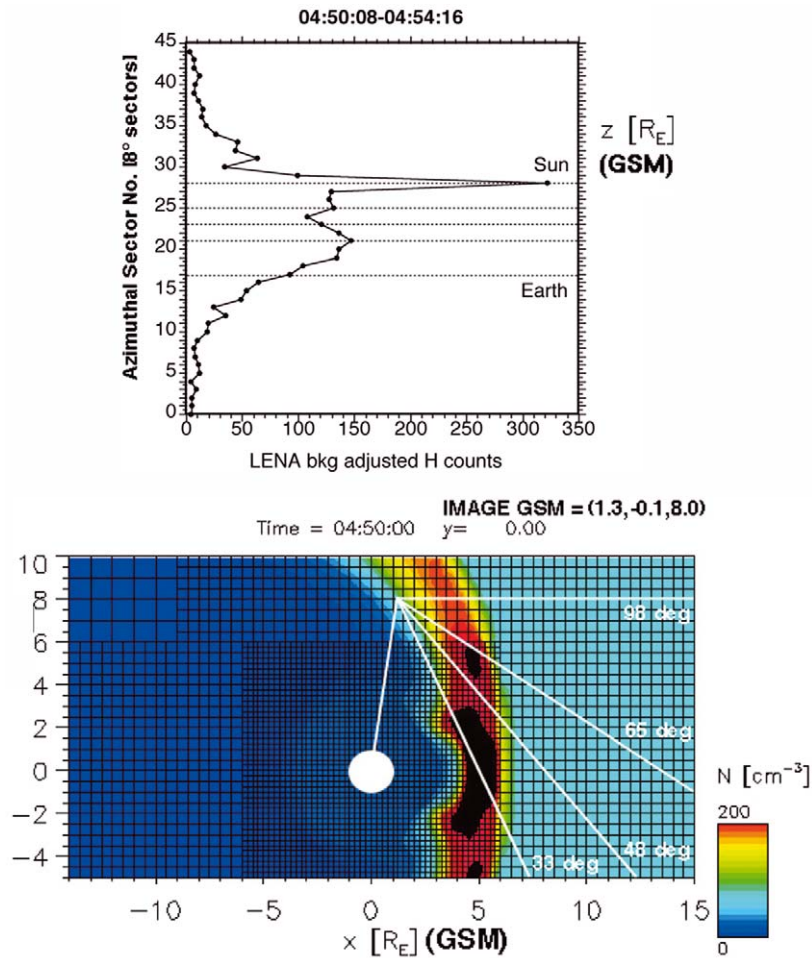
Figure 4. Comparison of LENA flux spin profile (left panel) with simulation structure for the 31 March 2001 CME event (right panel). The spacecraft position is indicated by the white vector originating at Earth's center. LENA imager look directions are indicated by white lines emanating form the spacecraft position, illustrating the features lying along the line of sight within the simulation of this event. Plasma density is color contoured within the simulation space.

the cusp density enhancement as well as the subsolar enhancement of densities relatively close to the Earth.

2.3. GEOCORONAL STRUCTURE

Comparisons with simulations of dayside magnetosheath emissions also reveal evidence of structure in the geocoronal gas distribution. Earlier studies of the geocorona based on UV scattering (Carruthers, 1976) have shown evidence for a day-night asymmetry of the geocorona. This was interpreted as a result of radiation
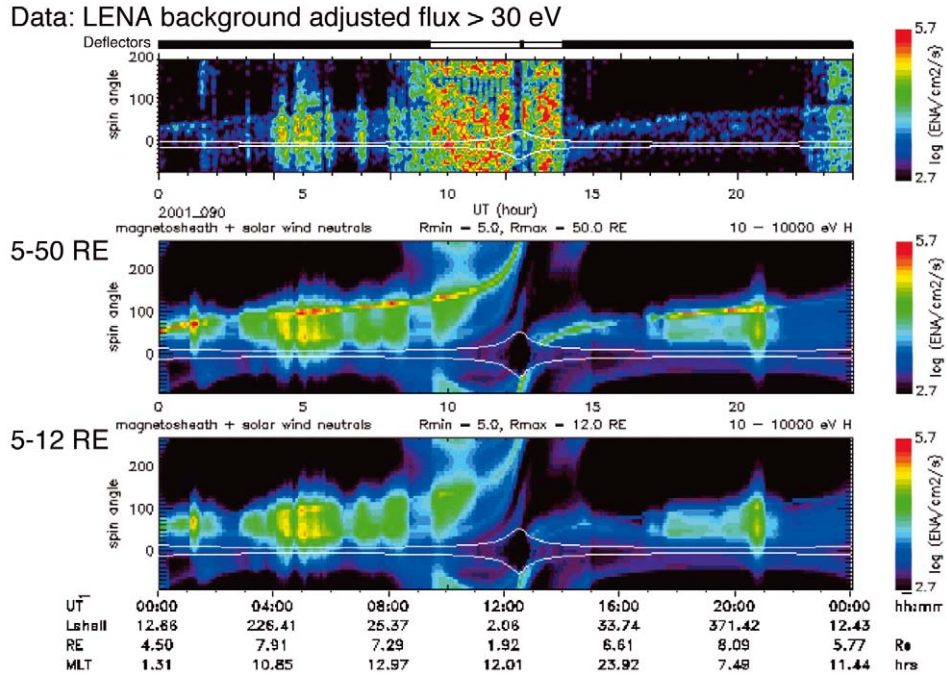
Figure 5. Full event comparison of observed LENA fluxes (upper panel) with simulated fluxes for the 31 March 2001 event (lower two panels). Line of sight integrations run from 5 to 50 R_E (middle panel), or from 5 to 12 R_E (lower panel), simulating a hard cutoff of the geocorona at 12 R_E.

pressure at the time. Another influence on the local geocoronal distribution may be the charge exchange losses of slow H atoms, when they give up an electron to a solar wind ion, and are suddenly picked up by the solar wind electromagnetic field (Bertaux and Blamont, 1973).

In Figure 5, we show a temporal comparison between LENA imager data and our simulation of magnetosheath LENA emissions, again for the 31 March 2001 event. Here we draw attention to the relative amount of LENA flux coming from the upstream solar wind, in comparison with that coming from the subsolar magnetosheath. The LOS integration extending out to 50 Re in the upstream direction produces a greater relative amount of direct solar wind LENA flux than is observed. In contrast, when an upper integration limit of 12 Re is adopted, the direct neutral solar wind is reduced to a relative level more consistent with that observed. The implication is that our geocoronal model (which is symmetric in local time), is excessively dense in the region beyond the mean magnetopause location. This apparent depletion of the upstream geocorona could be a result of radiation pressure, but it may also have a contribution from solar wind erosion of the geocorona in the upstream direction, which would be limited to the region beyond the magnetopause. We have not found any studies that have compared the geocoronal source

and loss rates in this region, but this would be a natural outgrowth of this LENA imaging work.

3. Geospheric Fast Neutral Atom Emission

3.1. RESPONSE TO SOLAR WIND PRESSURE INCREASES

Accompanying the neutral solar wind enhancements described above are closely associated enhancements of the flux of LENA being emitted from the Earth (Moore *et al.*, 2001; Fuselier *et al.*, 2001; Fuselier *et al.*, 2002). The LENA emission is thought to remotely represent plasma heating or acceleration processes that are producing ionospheric plasma outflows into the magnetosphere. These outflows appear to be directly driven by solar wind dynamic pressure but may also be influenced by other solar wind characteristics. They respond promptly to enhancements of solar wind intensity (within a few minutes). The response is sufficiently rapid to be incompatible with energy storage within the magnetosphere, but rather requires immediate extraction of energy from the solar wind. An example is shown in Figure 6, where a time sequence of LENA images is shown illustrating the variations of the LENA emission flux in correlation with solar wind fluctuations observed concurrently.

Comparison of the neutral emission flux with changes in the solar wind during an ion outflow event on 24 June 2000 indicates that changes in solar wind density (and therefore dynamic pressure) are associated with episodic bursts of ion outflow. Simultaneous images of the aurora from the IMAGE FUV Wideband Imaging Camera indicate that these episodic bursts on the duskside are associated with enhanced duskside auroral emissions. The pitch angle and charge exchange altitude for the ion outflow distributions were estimated by applying field line tracing in a model magnetic field and assuming that the outflow occurs in the auroral zone. The pitch angle information places constraints on the neutral atom images, indicating that the ion outflow observed on the duskside probably consists of high pitch angle conics and that field-aligned ion outflow from other parts of the oval cannot readily be observed from this particular IMAGE spacecraft location (Fuselier *et al.*, 2002).

Recent work has been directed toward phase-lagged cross-correlation analysis of observed LENA emissions and solar wind characteristics (Khan *et al.*, 2002). Owing to the wide range of altitudes from which IMAGE views the Earth, and the relatively small (i.e. unresolved) extent of the auroral regions emitting LENAs, it is important to account for the divergence of the flux away from these regions. When such correlations are done for the example shown in Figure 6, the correlation of LENA emissions with solar wind dynamic pressure is found to be optimal when the emissions are taken to diverge from a region located near 2 R_E geocentric radius. This suggests that the emissions being seen at very high altitudes originate from auroral acceleration regions known to operate in the 1 R_E altitude range, involving
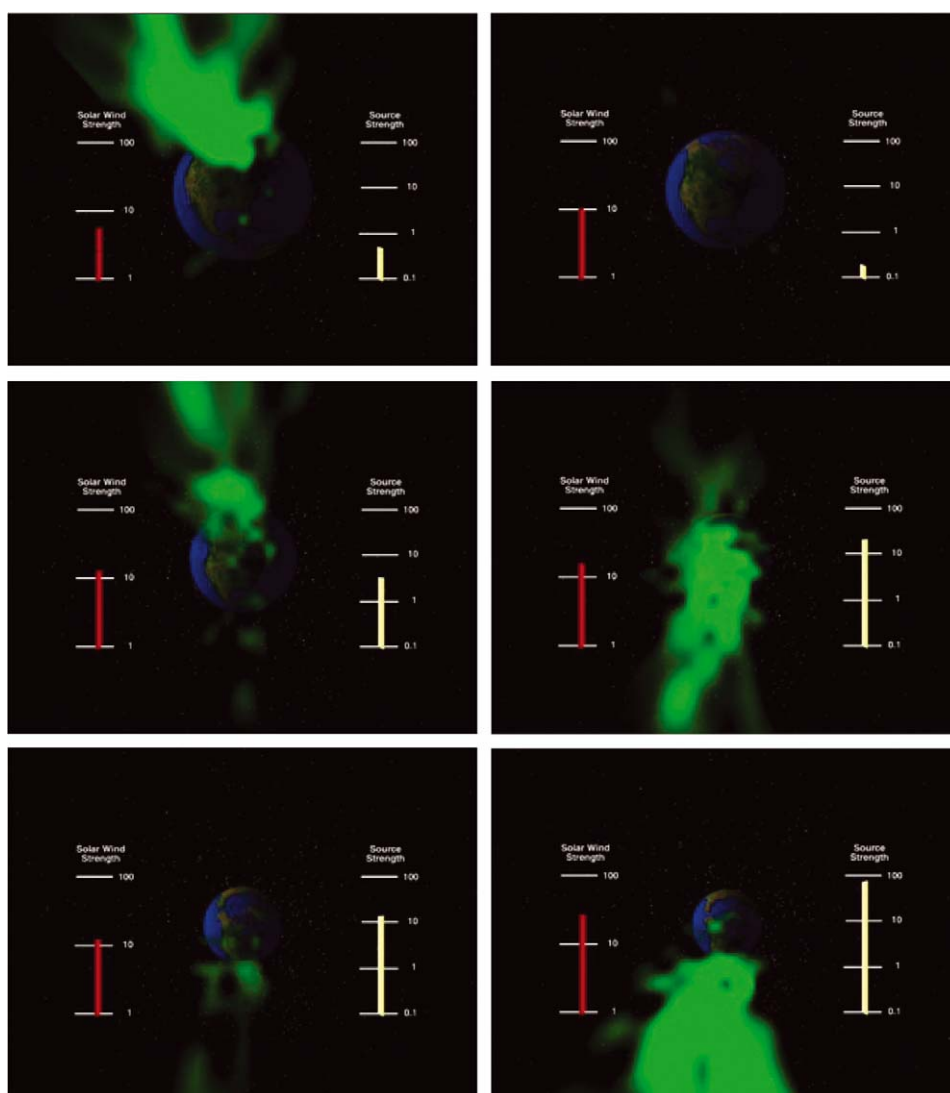
Figure 6. Time series of LENA fluxes observed at six times during the solar wind pressure enhancements of 24 June 2000. Also shown, in separate panels at left and right of the LENA fluxes, are the solar wind ram pressure in nPa, at the left, and the divergence-corrected LENA source strength (arbitrary units), on the right.

upward-directed parallel electric fields as a final stage of acceleration (McFadden, 1999).

3.2. LOW ALTITUDE HEATING

The elliptical orbit of the IMAGE spacecraft devotes the bulk of the observing time to high altitude imaging periods like those shown above. Once each orbit,

the spacecraft makes a fast pass over the southern polar regions with perigee at approximately 1000 km altitude. During these passes, a close up view of the LENA emissions is obtained. LENA fluxes often appear to be emitted from not only within the auroral zones, but from the entire polar cap region, and often extending into the subauroral regions. Moreover, there is often a flux feature that is coming from near the ram direction of the spacecraft, suggesting that the imager is responding to rammed neutral atoms of the exosphere.

There are some exceptions to the typical behavior, in which the LENA emissions appear to originate primarily from the auroral zone regions of energy input to the ionosphere. Figure 7 (left panel) displays a total LENA flux image from such a pass, during which the emission flux was relatively large, with some preference for the nightside auroral zone, which lies to the right in the image. Data from the Polar/TIDE instrument is plotted in the right panel, obtained at about 1 R_E altitude passing over the same southern polar cap region, at a time when the auroral zone was evidently still highly active in the production of ion outflows as well as LENA emissions.

The Polar spacecraft passed through the southern polar regions within a few hours of the LENA imaging observations, traversing regions conjugate with the southern auroral oval. At this time, it recorded the presence of a prolific region of auroral ion conic outflows, also emanating from the nightside auroral oval part of the pass.

When the fluxes of LENA are compared with the fluxes of ionospheric ions emitted within the ion conic outflow region for this event, it is found that they are of the same order of magnitude, approximately 10^8 cm^{-2}s^{-1}, when the ion fluxes are mapped back to the ionospheric topside region. The characteristic energy of the ion conics was 10-100 eV.

Figure 7 (bottom panel) shows a calculation of the fraction of upflowing O$^+$ converted to O atoms as a function of altitude. Neutral oxygen densities are from the MSIS model (Hedin, 1991) appropriate to the observed conditions and assume a charge exchange cross section of 2.5x10^{-15} cm^2. This result is compared with the neutral to ion ratio obtained from LENA and TIDE. The resulting source altitude estimate is bounded below by a ratio of 1 (i.e. no O$^+$ outflow) and the minimum calculated fractions. These bounds yield a minimum source altitude os 475 km and a maximum of 540 km from the TIDE/LENA results.

Several aspects of the behavior of LENA observed during perigee passes are surprising and somewhat disconcerting. First, the perigee images are much brighter than apogee images, brighter than can be accounted for by the divergence of the fluxes away from their source regions. The fluxes often appear to have an abrupt onset as the spacecraft approaches the polar cap region. Second, the LENA fluxes appear to come from all over the polar cap regions, in addition to the auroral zone. There are emissions that appear to come from lower latitude regions as well. Other characteristics of the perigee passes are more reassuring. For example, they are quite variable from orbit to orbit, and for the first few months of operation were
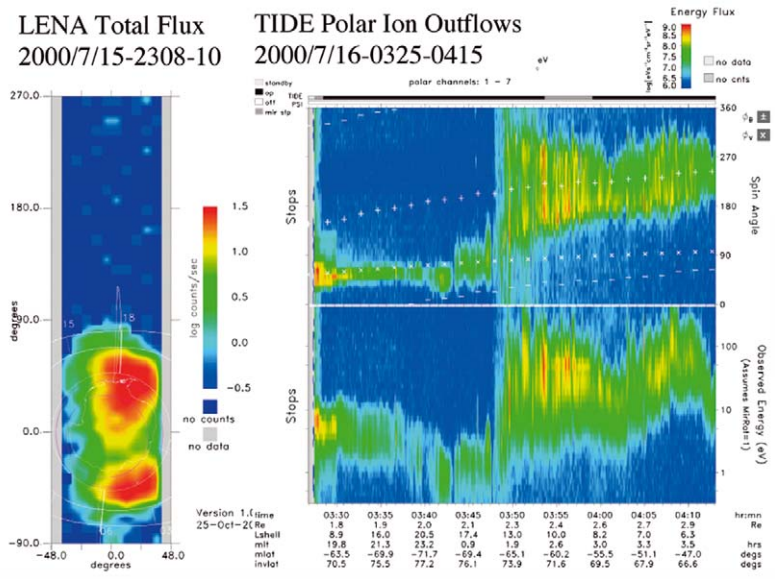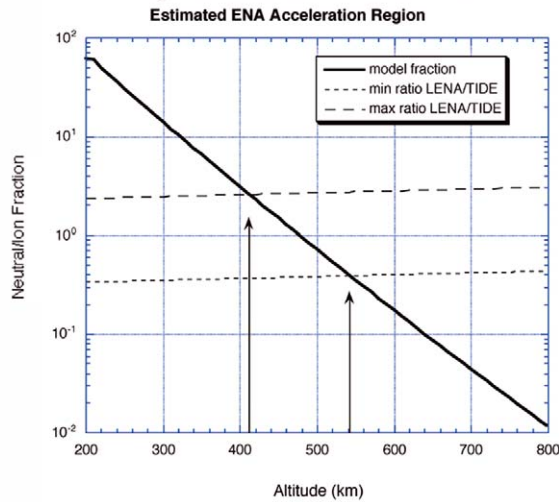
Figure 7. Active period LENA emission (left panel) and ion outflows (center panel) observed over the southern polar cap on 15–16 July 2000, with model results for neutral fraction of outflows (right panel) as a function of acceleration altitude. The LENA image (left panel) has the sun to the left, midnight to right. The auroral region is highlighted in red by 60–70° geomagnetic latitude circles. TIDE panels (center) show spin angle (upper) and energy (lower) distributions, with Polar ephemeris indicated at bottom.
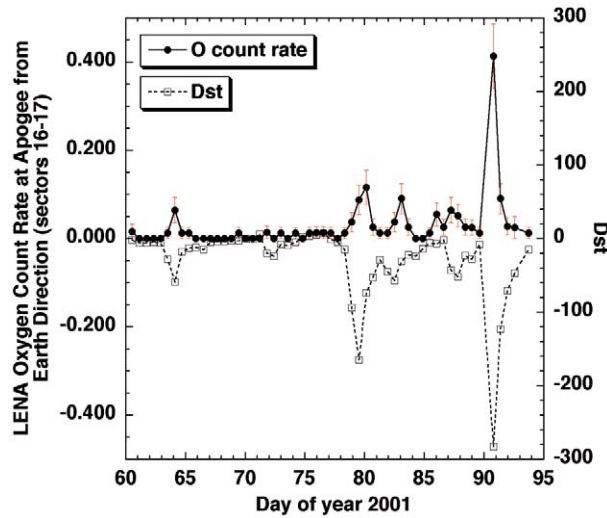
Figure 8. LENA oxygen at high altitudes for the month of March 2001 (upper trace, left Y axis), compared with the Dst index for the same period (lower trace, right Y axis).

quite well correlated with geomagnetic activity, as found by others (Yau *et al.*, 1985; Brandt *et al.* 2001). Often, a region of strong fluxes tracks the spacecraft ram direction through much of the perigee passes, suggesting that spacecraft motion is strongly influencing the flux distribution, and thereby implying that particle energies in the Earth frame are very low, possibly below gravitational escape velocity. LENA imager response is known to extend down to about 10 eV, and it may extend lower. Therefore, it is likely that LENA imager is observing oxygen atoms that are gravitationally bound to Earth (Fok *et al.*, this volume; Wilson *et al.*, 2003). Thus, the LENA imager is obtaining new observations of the heavy atom exosphere, revealing features that were previously unappreciated. Continued work comparing exospheric theory with LENA observations will produce important new knowledge about this interface between the magnetosphere and ionosphere.

3.3. LOW ENERGY RING CURRENT ATOM EMISSION

Because the useful LENA imager energy range extends up to a few keV owing to sputtering interactions on its conversion surface, it is capable of seeing neutral emission from the lowest energy ring current plasmas. It should and does in fact observe features very similar to those observed by the MENA imager in its lowest energy range. An example of these features is shown in Figure 8.

Here, our identification of this population as originating in the low energy ring current is bolstered by the fact that these fluxes are highly correlated with the Dst index, as shown in Figure 8. It should be noted that, as essentially a pinhole camera, albeit with a 1 cm^2 pinhole, the LENA imager is less sensitive than the MENA imager to these fluxes. However, it is reassuring to see that the same features
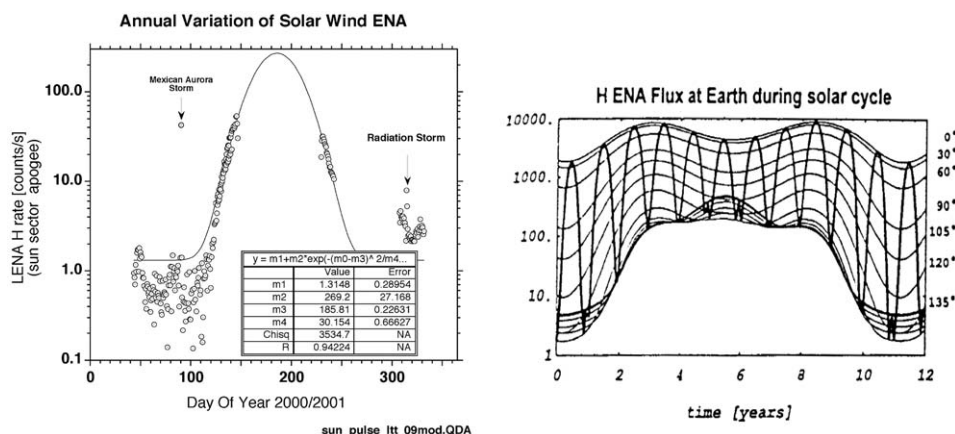
Figure 9. Comparison of observations and model of the neutral solar wind seasonal variation. LENA neutral solar wind hydrogen rate is plotted for the first year and a half of operations in the left panel. Model expectations from Bzowski *et al.*, (1996), are shown for an entire solar cycle in the right panel, thick sinusoidal trace. Thin traces indicate the corresponding offset angle from the upstream direction, as labeled at the far right.

are seen by two instruments of such fundamentally different operating principle. Another example of the LENA response to low energy ring current emissions is shown in Fok *et al.* (this volume).

4. Gas in the Inner Heliosphere

4.1. Neutral Solar Wind as Inner Heliospheric Probe

The three main charge exchange media in the inner solar system, dust, interstellar neutral gas, and planetary outgassing, produce variations of the neutral solar wind on distinct time scales. As pointed out earlier, the shorter term variations tend to be dominated by the interaction of the solar wind with the Earth's geocorona, simply because the degree of interaction is so strongly dependent on the dynamic pressure of the solar wind and hence its distance of penetration into the geocorona.

On longer time scales, the spatial structure of the heliospheric gas distribution becomes the controlling influence. After the first year of observing the neutral solar wind (Collier *et al.*, 2001) the signal was seen to have a very large amplitude seasonal variation that was being reproduced as the second year began. This in turn implied a pronounced spatial variation in the neutral gas column between Earth and Sun, as a function of season. As shown in Figure 9, the annual variation has amplitude almost two orders of magnitude, with neutral solar wind fluxes becoming low and erratic as the earth passes through the northern winter months, as compared with a large peak during northern summer months.

Such a variation is predicted by the model of Bzowski *et al.* (1996), who sought to evaluate the flux of fast hydrogen that would be incident on the Earth owing to such charge exchange of the solar wind. The model result is also shown for comparison in Figure 9. Accounting for both dust sources and interstellar neutral gas flow, including photoionization losses, this model predicts the distribution of neutral gas between the Sun and Earth as a function of Earth's orbital and solar cycle phases. Orbital phase is important owing to the relative interstellar neutral wind, originating from the interstellar upstream direction in the northern summer months. Solar cycle phase is important owing to variations of the solar EUV spectrum, controlling the photoionization of gas in the inner solar system. The competition between interstellar neutral advection and loss from photoionization and pickup in the solar wind produces an asymmetric distribution of interstellar gas between Sun and Earth, with a maximum in the summer months and minimum in the winter months. The large annual variation observed by LENA results in this model from the resultant large variation in the amount of neutral gas traversed by the solar wind, with a substantial column density enhancement extending sunward of Earth's orbit during summer months. The observations differ from the model, however, in that the peak of the neutral solar wind flux is shifted by approximately 30° of heliographic longitude from the interstellar gas upstream direction. Thus, these observations are being interpreted as resulting from a secondary stream of neutrals in the inner heliosphere (Collier *et al.*, 2003).

The amplitude of the modeled annual variation of neutral solar wind is determined by the amount of gas having its source in the inner solar system, and provides a basis for its estimation. This inner source is distributed more or less uniformly in season, producing a constant neutral solar wind component, above which the interstellar gas intrusion creates an enhancement. The principal source of such gas is thought to be the disk of dust in the inner solar system (Banks, 1971), whose source is most likely the disintegrated remains of small bodies traversing the inner solar system. Gas is most likely evolved from these dust grains through sputtering by solar wind ion impacts. Using the model of Banks, the flux of neutral solar wind seen in the winter minimum by LENA can be used to estimate the dust column density, yielding a result of $< 6 \times 10^{-19}$ cm^{-1}, which lies toward the low end of the range of previous estimates, extending over nearly five decades (Schwadron *et al.*, 2000; Banks, 1971). The LENA imager results (Collier *et al.*, 2002) are most nearly consistent with the estimates given therein, based on Zodiacal light. However, it should be noted that this estimate is highly dependent on the model of the sputter gas source, which is itself uncertain to some degree.

4.2. DIRECT OBSERVATIONS OF THE HE FOCUSING CONE AT 1 AU

LENA has also been able to directly observe the interstellar neutral gas atoms. The gas flow velocity has been measured (Witte *et al.*, 1993) to be relatively low (26 km/s). Thus, the energy of hydrogen (helium) in the spacecraft or Earth frame
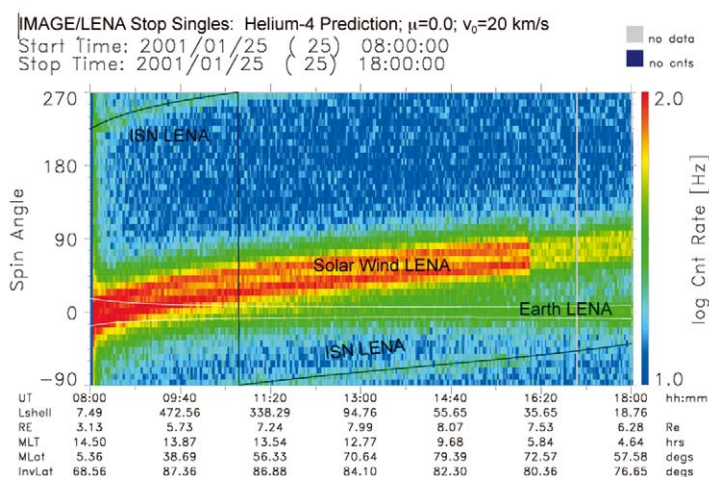
Figure 10. Interstellar neutral atom signal in the LENA summary plot format, with individual images collapsed in polar angle to form an angle-time spectrogram. The thin solid line is a fit to the location of the ISN LENA signal, for He^4, based on simple motion of interstellar neutral atoms through the solar system, with fit parameters as listed in the header.

(adding another 0–35 km/s, depending on season and orbital phase) would be at most 18 eV (70 eV). Since the LENA imager sensitivity falls off at such low hydrogen energies, and it has no nominal response to helium, detection of interstellar neutrals was somewhat speculative. Nevertheless, it was pointed out by Fuselier (personal communication) that the winter months would be the time to look for interstellar neutrals in LENA imager data, since their relative wind speed would maximize during that period, and they would be in the 90° wide field of view. Considering the sputtering response of the LENA conversion surface discussed above, it might be anticipated that a response to helium is definitely possible. In fact, a new signal appeared in the data in the first week of January 2001 (about a month later than anticipated, however) that had the anticipated characteristics of interstellar neutral atoms, as shown in Figure 10.

The flux gave maximal signal in the LENA stop singles rate, though there were enough events for TOF spectra to be obtained with integration (not shown here). These indicate that the majority of the interstellar neutral events were seen as H$^-$ ions by the LENA imager. To further substantiate the signal, the expected arrival spin directions of interstellar neutrals were calculated, including the deflections of H and He by the Sun. The LENA signal was then compared with this calculated position, yielding a best fit for He^4 that entered the solar system at 20 km/s in the sun frame, as shown in Figure 10. This indicates that we must be seeing sputtering of hydrogen from the conversion surface by incident helium atoms.

This identification is based largely on the gravitational interaction of helium and hydrogen with the sun. The radiation pressure on interstellar atoms varies inversely with the square of radius from the sun and is approximately equal to

the gravitational force on a hydrogen atom. The ratio of radiation force to oppositely directed gravitational force being denoted by μ, or about 0.8 for hydrogen (depending on solar UV flux and solar cycle phase), about 0.2 for helium (negligibly small) at solar minimum and nearly twice as large during solar maximum conditions appropriate here (e.g., Lallement, 1999). This is a very reasonable result when considering that interstellar hydrogen densities at Earth downstream of the sun are expected to be very small, especially in view of the LENA confirmation of a large amplitude seasonal modulation of neutral solar wind. Owing to its greater net gravitation-radiation interaction, interstellar helium is expected to form a gravitational "focusing cone" that should produce a peak density at the downstream position of the Earth's orbit around the sun. Evidence for the He cone is seen in heliospheric pickup ions (Gloeckler and Geiss, 2001). The hydrogen cone would form well beyond the Earth's orbit for any credible value of μ, and defocusing (net repulsion) would occur for H at μ values typical of solar maximum conditions appropriate here.

At this writing, a second season of direct interstellar neutral observations has been acquired and we are entering a third season. The spatial distribution is to first order consistent with what was observed during the prior year, but our sensitivity to them appears to have declined noticeably. For both seasons, the peak of the interstellar He signal occurs later than the interstellar gas downstream position by one month of Earth orbital motion (Collier *et al.*, 2003). This is under active investigation at this time, with the working hypothesis that there is a secondary stream of interstellar neutrals, possibly produced by the heliospheric boundary interaction, that dominates in the inner heliosphere owing to a higher velocity.

The heliospheric gas populations that create LENA from various ionized particle populations are summarized in Figure 11. First, we have the terrestrial exosphere and escaping geocorona that charge exchanges, producing LENA, with ionospheric and magnetospheric plasmas. Next, we have a relatively slow interstellar wind, somewhat slower than the Earth's orbital motion of 30 km/s. Photoionization and charge exchange with the solar wind convert these atoms to ions and they are carried off by the solar wind, largely eliminating this flow from the innermost solar system. Gravitational deflections affect the distributions of gas in the wake region downstream. Hydrogen is expected to be strongly defocused during solar maximum activity phase, while for helium a focusing cone forms at or inside the Earth's orbit so that a distinct enhancement is observed in downstream direction. Finally, an inner solar system dust population produces gas sputtered by solar wind ions. This population is independent of season, leading to a baseline neutral solar wind component much smaller than that produced by interstellar neutral gas in the upstream direction.
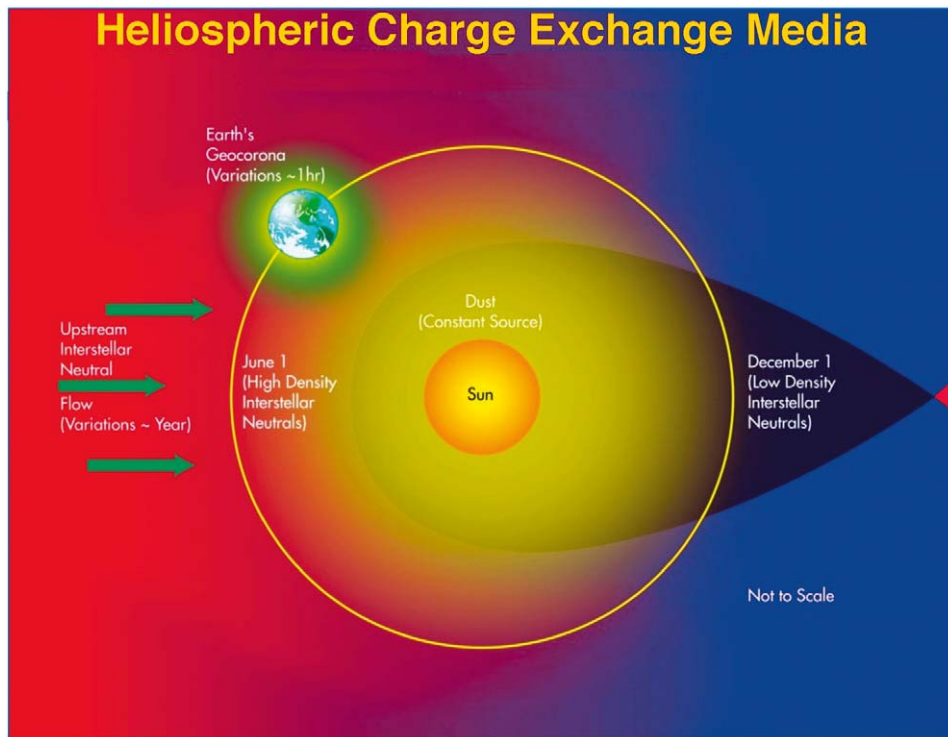
Figure 11. Three heliospheric charge exchange media relevant to LENA production in the inner solar system: Earth's geocorona, interstellar neutral gas, and gas from inner solar system dust.

5. Conclusions

In conclusion, our experience with low energy neutral atom detection and imaging on the IMAGE spacecraft has led to a number of advancements in our understanding of the low energy partially ionized plasmas of the Earth, sun and interplanetary medium, including the interstellar neutral gas in our solar system. To summarize:

- We have been able to observe solar wind neutral atoms from inside the magnetosphere.
- We've been able to use neutral atom emissions to reveal the magnetosheath, with cusp-related structures, and evidence of upstream erosion of the geocorona.
- We found that ionospheric outflow responds promptly to solar wind dynamic pressure variations, observing emitted LENA at or near IMAGE apogee of $\sim 8R_E$.
- We infer a plasma heating source below 1000 km altitude for the larger LENA emission flux events observable in perigee passes.
- We have inferred a newly-appreciated orbiting population of superthermal exospheric oxygen, generated by low altitude auroral plasma heating processes.

- We measured the annual variation of the neutral solar wind as a probe the interstellar gas and dust in the inner solar system.
- We directly observed a feature resembling the interstellar neutral helium focusing cone at 1 AU.

LENA imaging has thus been proven an effective new tool for the study of the interplanetary medium and its interaction with the magnetosphere, even from inside the magnetosphere. Considerable additional work remains to be done to investigate the hot exospheric oxygen and the observed offsets in interstellar neutral gas phenomena.

Acknowledgements

References

Bertaux, J.L. and Blamont, J.E.: 1973, 'Interpretation of OGO-5 Lyman alpha measurements in the upper geocorona', *J. Geophys. Res.* **78**, 80.

Brandt, P.C:son, Barabash, S., Roelof, E.C. and Chase, C.J.: 2001, 'ENA Imaging at Low Altitudes From the Swedish Microsatellite Astrid: Observations at low (<10 keV) energies}', **106**,(A11), p. 24663.

Burch, J.L. et al.: 26 Jan 2001, 'Views of Earth's Magnetopshere with the IMAGE Satellite', *Science*, **291**, p. 619.

Carruthers, G.R., Page, T. and Meier, R.R.: 1976, 'Apollo 16 Lyman alpha imagery of the hydrogen geocorona', *J. Geophys. Res.* **81**, p. 1664.

Collier, Michael, Thomas, R., Moore, E., Ogilvie, Keith W., Chornay, Dennis, Keller, J.W., Boardsen, S., Burch, James, Marji, B.El., Fok, M.-C., Fuselier, S.A. Ghielmetti, A.G., Giles, B.L., Hamilton, D.C., Peko, B.L., Quinn, J.M., Roelof, E.C., Stephen, T.M., Wilson, G.R. and Wurz, P.: 2001, 'Observations of neutral atoms from the solar wind', *J. Geophys. Res.* **106**, 24,893–24,906.

Collier, M.R., Moore, T.E., Ogilvie, K., Chornay, D.J., Keller, J., Fuselier, S., Quinn, J., Wurz, P., Wuest, M. and Hsieh, K.C.: 2002, 'Dust in the wind: The dust geometric cross section at 1AU based on neutral solar wind observations', Solar Wind 10 Proceedings, 2003.

Collier, M.R., Moore, T.E., Simpson, D.G., Roberts, A., Szabo, A., Fuselier, S., Wurz, P., Lee, M.A. and Tsurutani, B.T.: 2003, 'Adv. In Space Res., Proceedings of COSPAR 2002', in review.

Fok, M.-C., Moore, T.E., Wilson, G.R., Perez, J.D., Zhang, X., Brandt, PC:son, D G Mitchell, D.G., Roelof, E.C., Jahn, J.M., Pollock, C.J., Wolf, R.A.: 2003, 'Global ENA IMAGE Simulations', this volume.

Fuselier, S.A., Ghielmetti, A.G., Moore, T.E., Collier, M.R. *et al.*: 2001, 'Ion outflow observed by IMAGE: Implications for source regions and heating mechanisms', *Geophys. Res. Lett.* Vol. 28, **6**, p. 1163.

Fuselier, SA, Collin, H.L., Ghielmetti, A.G., Claflin, E.S., Moore, T.E., Collier, M.R., Frey, H. and Mende, S.B.: 2002, 'Localized ion outflow in response to a solar wind pressure pulse', *J. Geophys. Res.*, **107**(A8), SMP 26-1, 2002.

Gloeckler, G. and Geiss, J.: 2001, 'Heliospheric and interstellar phenomena deduced from pickup ion observations', *Space Sci. Rev.* **97**, p. 169.

Groth, C.P.T., Zeeuw, D.L., Gombosi, T.I. and Powell, K.G.: 2000, 'Global three-dimensional MHD simulation of a space weather event: CME formation, interplanetary propagation, and interaction with the magnetosphere', *J. Geophys. Res.* **105**, 25053–25078.

Hedin, A.E.: 1991, 'Extension of the MSIS Thermospheric Model into the Middle and Lower Atmosphere', *J. Geophys. Res.* **96**, 1159.

Holzer, T.E.: 1977, 'Neutral hydrogen in interplanetary space', *Revs. Geophys. Space Phys.* **15**, p. 467.

Khan, H., Collier, M.R. and Moore, T.E.: 2002, 'Observations of ionospheric outflow events as measured by the Low Energy Neutral Atom (LENA) imager on IMAGE in association with variations in the solar wind', *EOS Trans. AGU*, **83**(47), Fall Meet. Suppl., Abstract SA12AA-08, 2002.

Lallement, R.: 1999, 'Global Structure of the Heliosphere: Optical Observations, Solar Wind 9', Habbal *et al.* eds., AIP 471, p. 205–210.

McFadden, J.P., Carlson, C.W. and Ergun, R.E.: 1999, 'Microstructure of the auroral acceleration as observed by FAST', *J. Geophys. Res.* **104**(A7), p. 14,453.

Mitchell, D.G., *et al.*, this volume.

Moore, T.E., Lundin, R. *et al.*: 1999, 'Source processes in the high latitude ionosphere', *Space Sci. Revs* **88**(1–2), p. 7.

Moore, T.E., Chornay, D.J., Collier, M.R., Herrero, F.A., Johnson, J., Johnson, M.A., Keller, J.W., Laudadio, J.F., Lobell, J.V., Ogilvie, K.W., Rozmarynowski, P., Fuselier, S.A., Ghielmetti, A.G., Hertzberg, E., Hamilton, D.C., Lundgren, R., Wilson, P., Walpole, P., Stephen, T.M., Peko, B.L., Van Zyl, B., Wurz, P., Quinn, J.M., Wilson, G.R.: 2000, The Low Energy Neutral Atom Imager for IMAGE, *Space Sci. Revs*, **91**, 155–195.

Moore, T.E. , Collier, M.R., Burch, J.L., Chornay, D.J. *et al.*: 2001, 'Low Energy Neutral Atoms in the Magnetosphere', *Geophys. Res. Lett.* Vol. 28, **6**, p. 1143.

Pollock, C.J. *et al.*, this volume.

Rairden, R.L., Frank, L.A. and Craven, J.D.: 1986, 'Geocoronal Iimaging with Dynamics Explorer', *J. Geophys. Res.* **91**, p. 13613.

Schwadron, N.A., Geiss, J., Fisk, L.A., Gloeckler, G., Zurbuchen, T.H. and von Steiger, R.: 2000, 'Inner source distributions: Theoretical interpretation, implications, and evidence for inner source protons', *J. Geophys. Res.* **105**, p. 7465.

Scudder, J.D.: 1992, 'The cause of the coronal temperature inversion of the solar atmosphere and the implications for the solar wind, in *Solar Wind Seven*, ed. by Marsch, E. and Schwenn, R., p. 103, Pergammon Press, Oxford.

Suess, S.T.: 1990, 'The Heliopause', *Revs. Geophys.*, **28**(1), p. 97.

Wilson, G.R., Moore, T.E. and Collier, M.R.: 2003, 'Low energy neutral atoms observed near the Earth', *J. Geophys. Res.* **108**(A4), 10.1029/2002JA009643, 3 April 2003.

Witte, M., Rosenbauer, H., Banaszkiewicz, M. and Fahr, H.: 1993, 'The Ulysses neutral gas experiment: Determination of the velocity and temperature of the interstellar medium', *Adv. Space Res.* **13**(6), p. 121.

Yau, A.W., Shelley, E.G., Peterson, W.K., Lenchyshyn, L.: 1985, 'Energetic Auroral and Polar Ion Outflow and DE 1 Altitudes: Magnitude, Composition, Magnetic Activity Dependence, and Long-Term Variations', *J. Geophys. Res.* **90**, 8417.